

**PIEZOMAGNETIC AND ULTRASONIC PROPERTIES  
OF THE Fe-Cu-Nb-Si-B METALLIC GLASS AFTER HEAT-TREATMENT**

**Z. KACZKOWSKI\*, L. MAŁKIŃSKI\* AND M. MÜLLER\*\***

\*Institute of Physics Polish Academy of Sciences  
(02-668 Warszawa, Al. Lotników 32/46)

\*\*Institute of Solid State and Material Research  
(0-8027 Dresden, Helmholtzstr. 20, Germany)

An  $\text{Fe}_{73.5}\text{Cu}_1\text{Nb}_3\text{Si}_{16.5}\text{B}_6$  alloy was cast as an initially amorphous ribbon. The samples about 50–51 mm long and 4 mm wide were cut out from the 10 mm wide and about 15  $\mu\text{m}$  thick ribbon and annealed at the temperatures over 300°C (to 550°C) in the transverse magnetic field  $H_{\perp}$  and also without magnetic field ( $H=0$ ). Before nanocrystallization this alloy exhibits the saturation magnetostriction equal to  $(20-23) \times 10^{-6}$ . The annealing at the temperatures over 400°C in the transverse magnetic field increases the maximum value of the magnetomechanical coupling coefficient ( $k_m$ ) from 0.10–0.15 (for as quenched state) to over 0.45. The magnetic anisotropy, introduced during the heat-treatment in the transverse magnetic field, is responsible for the predominant vector rotation mechanism which increases the magnetomechanical coupling and  $\Delta E$ -effect.

**1. Introduction**

FINEMETs or Yoshizawa's alloys, i.e. iron-rich alloys with an ultrafine grain structure (with a diameter equal to 10–20 nm) are known as nanocrystalline materials [1–12]. These alloys after nanocrystallization are excellent soft magnetic materials, but before the crystallization they exhibit a saturation magnetostriction equal to  $(20-23) \times 10^{-6}$  [1, 5–8] and they may be used as good piezomagnetic materials [9–11].

**2. Experimental**

An  $\text{Fe}_{73.5}\text{Cu}_1\text{Nb}_3\text{Si}_{16.5}\text{B}_6$  alloy was cast as an initially amorphous ribbon [5–11]. The samples about 50–51 mm long and 4 mm wide were cut out from the 10 mm wide and about 15  $\mu\text{m}$  thick ribbon and annealed at the temperatures over 300°C (to 550°C)

in the transverse magnetic field ( $H_1 = 650$  kA/m) and also without magnetic field ( $H=0$ ) [9–11]. In the first series the strips nos. 1–3 were annealed at the temperature of  $350^\circ\text{C}$  for 1/2 h in a transverse magnetic field. Next, the samples nos. 1 and 2 were annealed at a temperature of  $400^\circ\text{C}$  for 4 and 6 hours without magnetic field [9, 10]. In the second series these samples and the next one (i.e. nos. 1–4) were annealed at  $500^\circ\text{C}$  for 1/2 in  $H_1$  and  $H=0$ , and at last at  $550^\circ\text{C}$  for 1/2 h without a magnetic field. In the third series next 11 samples (nos. 5–16) were annealed in transverse magnetic field for 1 h in the temperature range from 300 up to  $500^\circ\text{C}$  [11]. The characteristics of the magnetomechanical coupling coefficient ( $k$ ) [13] and of the elasticity moduli at constant magnetic field ( $E_H$ ) and at constant magnetic induction ( $E_B$ ) versus magnetic bias field ( $H$ ) were obtained using the resonance-antiresonance method [13–15]. The magnetomechanical coupling coefficient ( $k$ ) was determined from the resonant ( $f_r$ ) and antiresonant ( $f_a$ ) frequencies of the half-wave resonators, i.e. of the strip-shape samples [14, 15]

$$k^2 = \frac{\pi^2 f_a^2 - f_r^2}{8 f_a^2} \quad (1)$$

The moduli of elasticity at the constant magnetic field ( $E_H$ ) and at the constant induction ( $E_B$ ) were calculated also from these resonant and antiresonant frequencies, respectively, i.e.:

$$E_H = c_H^2 \rho \approx 4l^2 f_r^2 \rho \quad (2)$$

and

$$E_B = c_B^2 \rho \approx 4l^2 f_a^2 \rho \quad (3)$$

where  $l (= \lambda/2)$  is the length of the half-wave resonator ( $l = 50$  or  $51$  mm),  $\rho$  is density ( $\rho = 7.2$  Mg/m<sup>3</sup>) and  $c_H$  and  $c_B$  are the ultrasound velocities at constant magnetic field  $H$  and at constant magnetic induction  $B$  respectively. The resonant frequencies were ranging from 30 to 52 kHz. The amplitude of the AC magnetic field was equal to 1–3 A/m. The characteristics of the impedance moduli are presented in Figures 1–3.

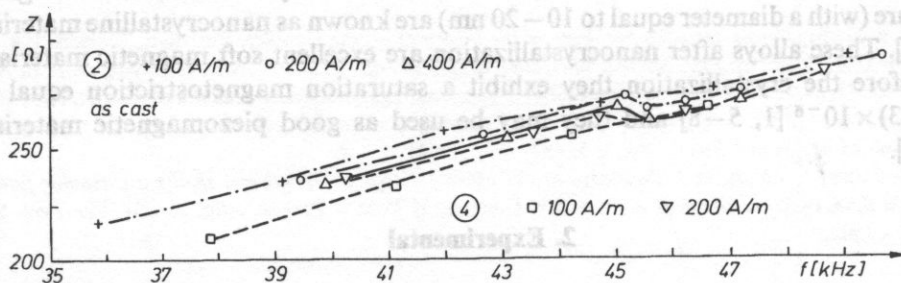


Fig. 1. Impedance ( $Z$ ) vs. frequency ( $f$ ) for samples no. 2 [10] and no. 4 in as-quenched state for magnetic bias field equal to 100, 200 and (400 A/m).

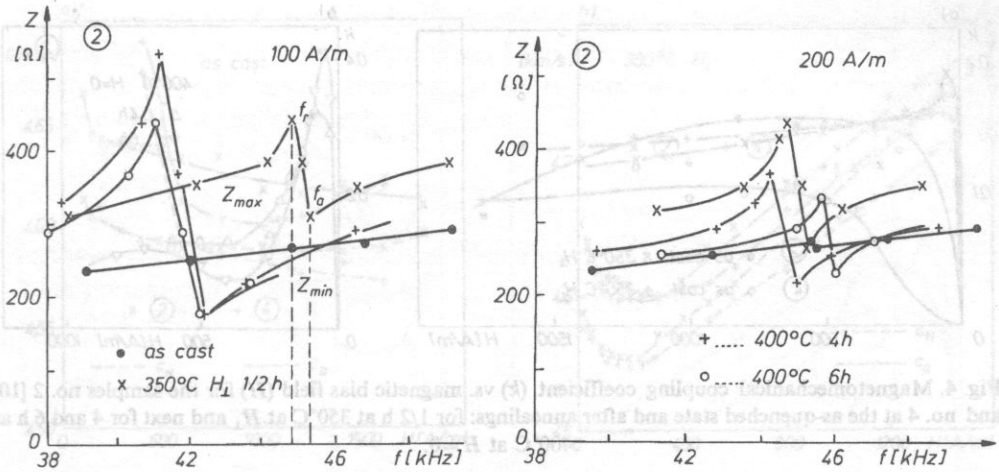


Fig. 2. Impedance ( $Z$ ) vs. frequency ( $f$ ) for sample no. 2 in as-quenched state and after annealing at transverse magnetic field ( $H_{\perp} = 650 \text{ kA/m}$ ) for 1/2 h at  $350^{\circ}\text{C}$  and for 4 and 6 h without magnetic field at  $400^{\circ}\text{C}$  for magnetic bias field equal to 100 and 200 A/m [9].

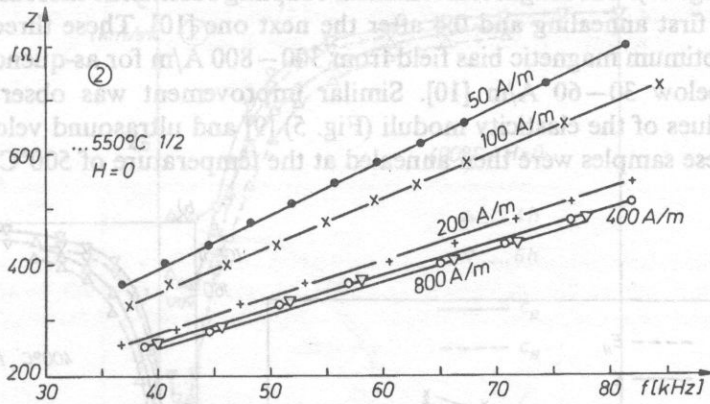


Fig. 3. Impedance ( $Z$ ) vs. frequency ( $f$ ) for sample no. 2 after last annealing for 1/2 h at  $550^{\circ}\text{C}$  and  $H=0$ .

Quasistatic hysteresis loops of magnetic induction ( $B$ ) were measured and from these loops the coercive force ( $H_c$ ) was determined [11]. Dynamical reversible magnetic permeability ( $\mu$ ) at the frequency of 10 kHz and the small amplitude of the magnetic field equal to 1A/m was measured versus quasistatic field [11].

### 3. Results and discussion

The annealing at the temperature of  $350^{\circ}\text{C}$  in the transverse magnetic field increases the maximum value of the magnetomechanical coupling coefficient ( $k$ ) from

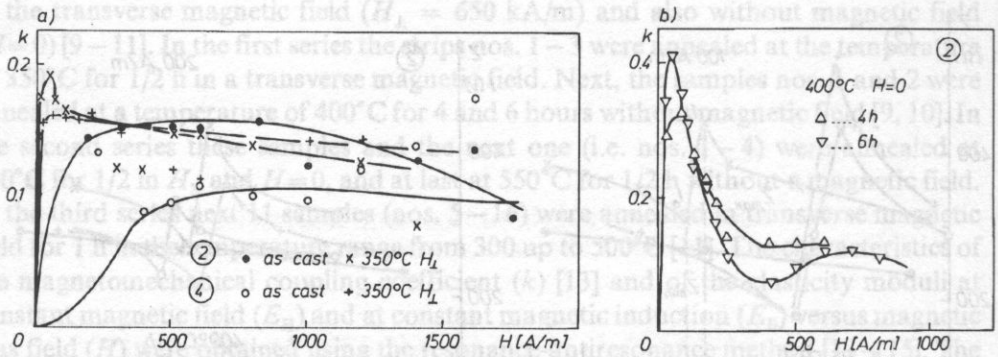


Fig. 4. Magnetomechanical coupling coefficient ( $k$ ) vs. magnetic bias field ( $H$ ) for the samples no. 2 [10] and no. 4 at the as-quenched state and after annealings: for 1/2 h at 350°C at  $H_L$  and next for 4 and 6 h at 400°C at  $H=0$ .

0.10–0.15 to 0.15–0.19 (fig. 4a) [10]. The next annealings at the temperature of 400°C for 4 and 6 h without external magnetic field improved the piezomagnetic properties (Fig. 4b). The magnetomechanical coupling coefficient exceeds the value of 0.3 after the first annealing and 0.4 after the next one [10]. These three annealings shifted the optimum magnetic bias field from 300–800 A/m for as-quenched state to the values below 30–60 A/m [10]. Similar improvement was observed for the minimum values of the elasticity moduli (Fig. 5) [9] and ultrasound velocities (Figs. 6 and 7). These samples were then annealed at the temperature of 500°C for 1/2 h in

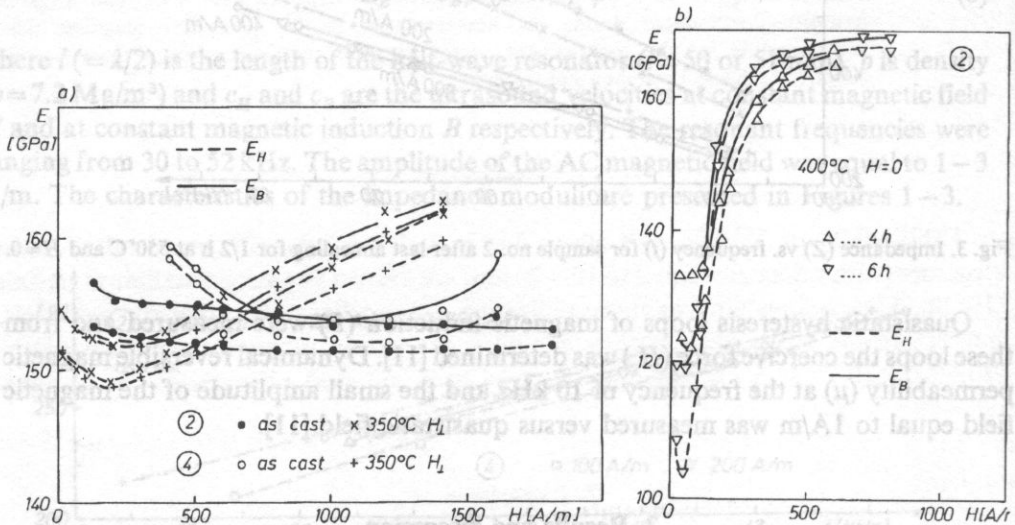


Fig. 5. Moduli of elasticity at constant magnetic field ( $E_H$ ) and at constant induction ( $E_B$ ) vs. magnetic bias field ( $H$ ) for the as-quenched and annealed for 1/2 h at 350°C in  $H_L$  samples (nos. 2 [9] and 4) and next annealed for 4 and 6 h at 400°C at  $H=0$ .

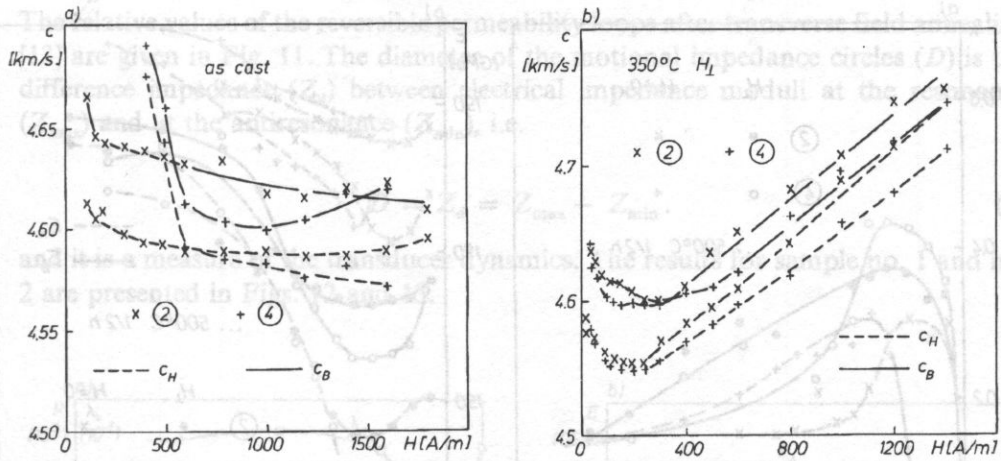


Fig. 6. Ultrasound velocities at constant magnetic field ( $c_H$ ) and at constant induction ( $c_B$ ) vs. magnetic bias field ( $H$ ) for the as-quenched and annealed for 1/2 h at 350°C in  $H_{\perp}$  samples nos. 2 and 4.

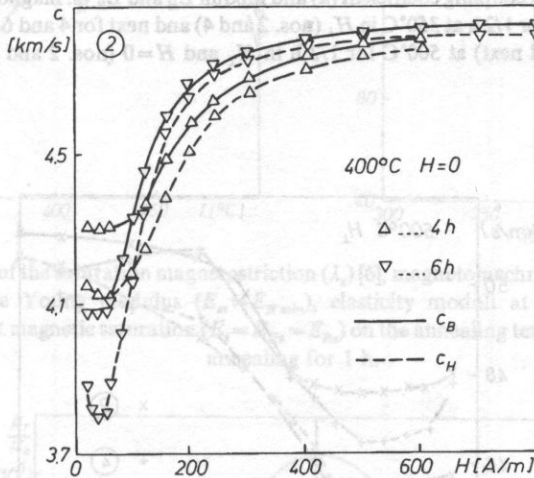


Fig. 7. Ultrasound velocities at constant magnetic field ( $c_H$ ) and at constant induction ( $c_B$ ) vs. magnetic bias field ( $H$ ) for the as-quenched and annealed for 1/2 h at 350°C in  $H_{\perp}$  4 and next annealed for 4 and 6 h at 400°C at  $H=0$  samples nos. 2 and 4.

the transverse magnetic field ( $H_{\perp}$ ) and next without a magnetic field at 500 and 550°C for 1/2 h (Figs. 8, 9 and 3).

Summarized results from the third series of the investigations are presented in Fig. 10 [13]. The annealing temperatures starting from 300°C were increased to 320, 340, 360, 380, 400, 420, 440, 460, 480 and 500°C. An exception is the saturation magnetostriction ( $\lambda_s$ ) for which the results were taken from the other papers [6–8].

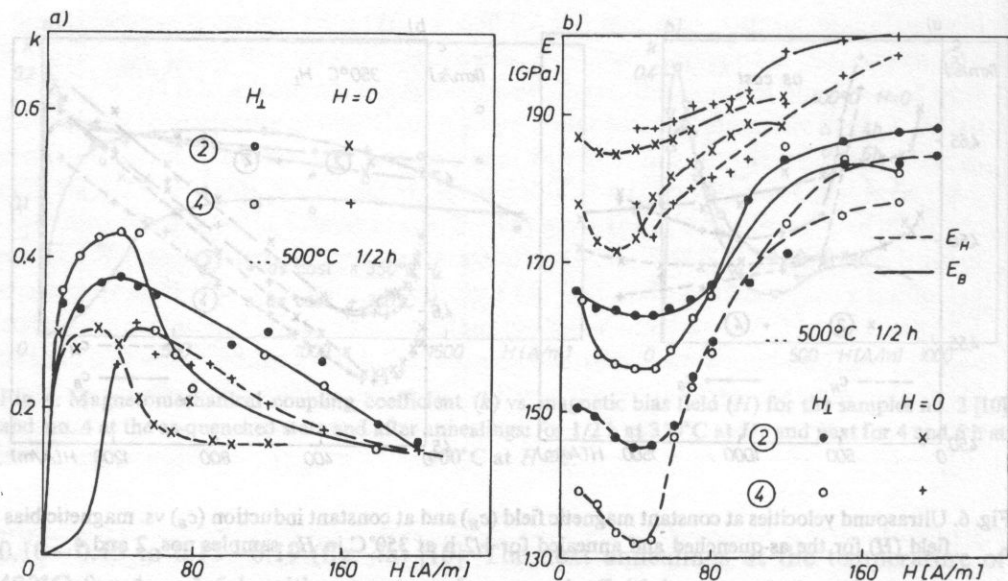


Fig. 8. Magnetomechanical coupling coefficient ( $k$ ) and moduli  $E_H$  and  $E_B$  vs. magnetic bias field ( $H$ ) for two samples after annealings: for 1/2 h at 350°C in  $H_{\perp}$  (nos. 2 and 4) and next for 4 and 6 h at 400°C at  $H=0$  (no. 2) and next at 500°C for 1/2 h in  $H_{\perp}$  and  $H=0$  (nos. 2 and 4).

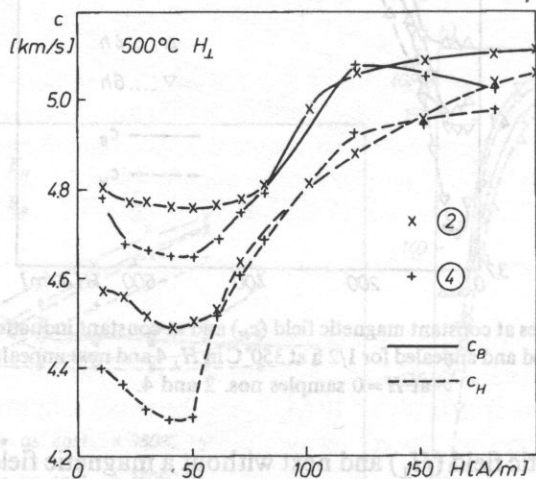


Fig. 9. Ultrasound velocities at constant magnetic field ( $c_H$ ) and at constant induction ( $c_B$ ) vs. magnetic bias field ( $H$ ) for two samples after annealings: for 1/2 h at 350°C in  $H_{\perp}$  (nos. 2 and 4) and next for 4 and 6 h at 400°C at  $H=0$  (no. 2) and next at 500°C for 1/2 h in  $H_{\perp}$  and  $H=0$  (nos. 2 and 4).

The relative values of the reversible permeability loops after transverse field annealing [13] are given in Fig. 11. The diameter of the motional impedance circles ( $D$ ) is the difference impedance ( $Z_d$ ) between electrical impedance moduli at the resonance ( $Z_{max}$ ) and at the antiresonance ( $Z_{min}$ ), i.e.

$$D = Z_d = Z_{max} - Z_{min} \tag{4}$$

and it is a measure of the transducer dynamics. The results for sample no. 1 and no. 2 are presented in Figs. 12 and 13.

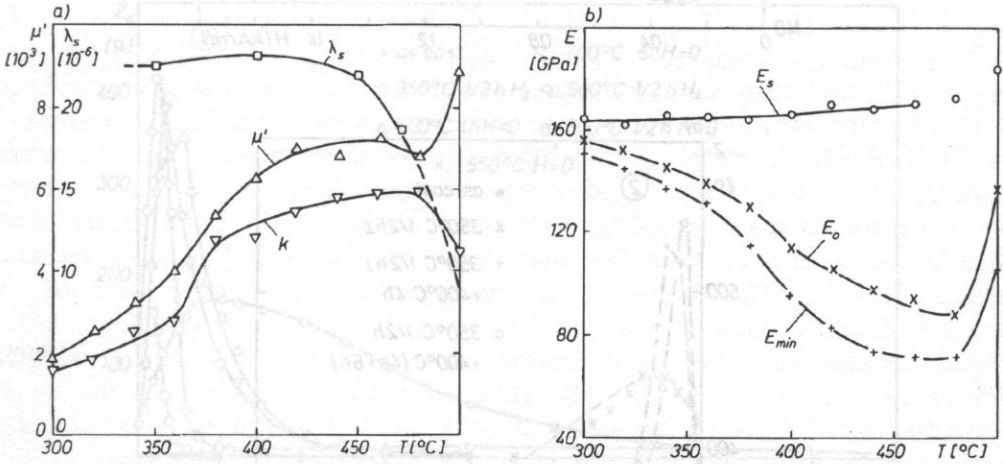


Fig. 10. Dependences of the saturation magnetostriction ( $\lambda_s$ ) [6], magnetomechanical coupling coefficient ( $k$ ), relative values of the Young modulus ( $E_m = E_{H \min}$ ), elasticity moduli at the demagnetization state ( $E_0 = E_{H_0} = E_{B_0}$ ) and at magnetic saturation ( $E_s = E_{H_s} = E_{B_s}$ ) on the annealing temperature of transverse field annealing for 1 h.

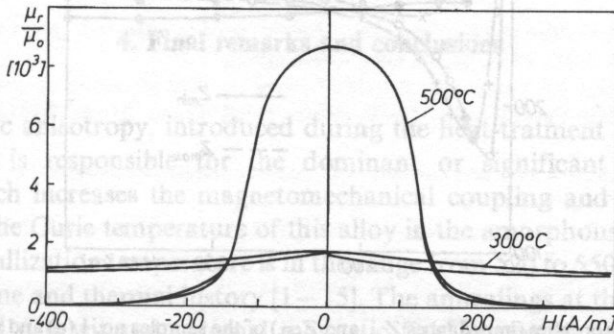


Fig. 11. Reversible ac permeability loops after transverse field annealings for 1 h at the temperature of 300 and 500°C.

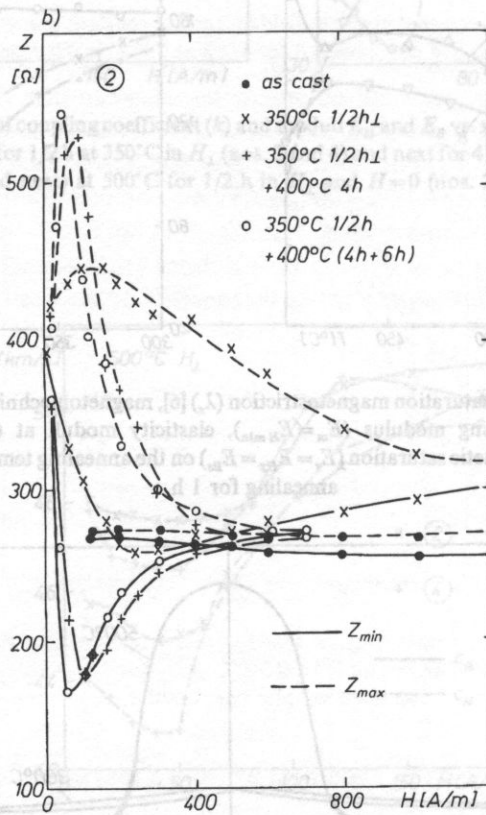
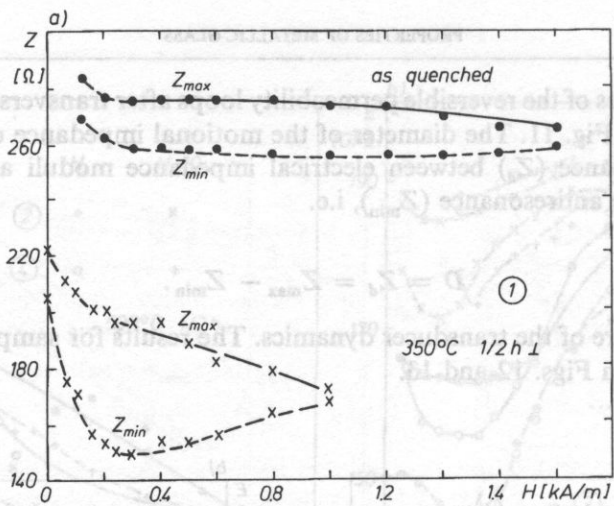


Fig. 12. Dynamical properties (impedances  $Z_{max}$  and  $Z_{min}$ ) of the samples no. 1 (a) and no. 2 (b) vs. magnetic bias field ( $H$ ) for as-casted state and after different heat treatment.



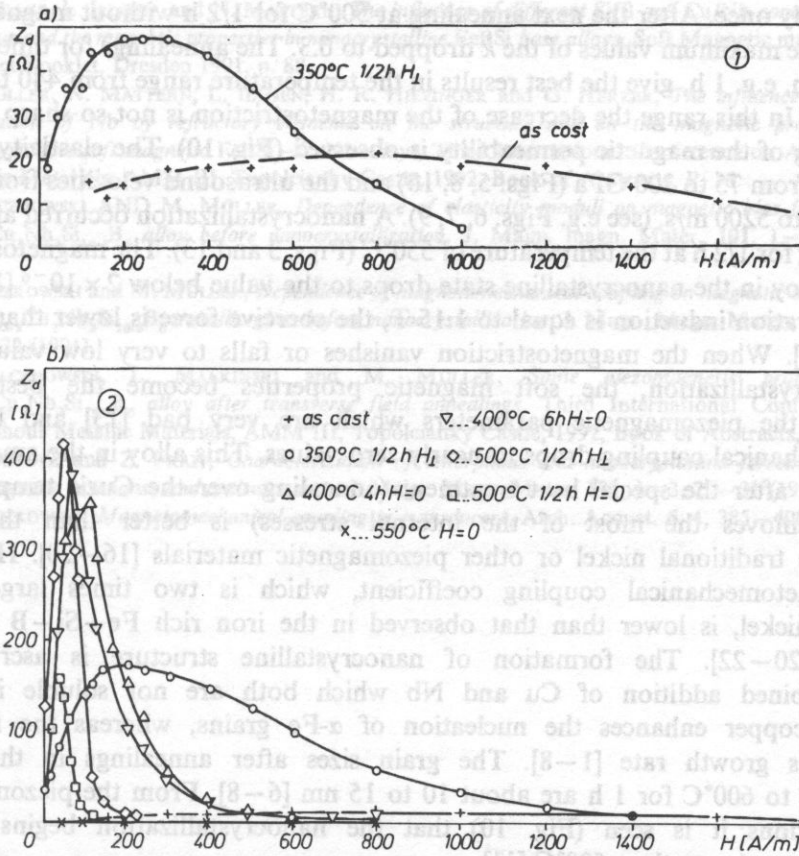


Fig. 13. Motional impedance  $Z_d = Z_{max} - Z_{min}$  of the samples no. 1 (a) and no. 2 (b) vs. magnetic bias field ( $H$ ) for as-casted state and after different heat treatment.

#### 4. Final remarks and conclusions

The magnetic anisotropy, introduced during the heat-treatment in the transverse magnetic field, is responsible for the dominant or significant vector rotation mechanism which increases the magnetomechanical coupling and  $\Delta E$  or  $\Delta c$  effect (Figs. 4–10). The Curie temperature of this alloy in the amorphous state is equal to 320°C and crystallization temperature is in the range from 520 to 550°C depending on the annealing time and thermal history [1–15]. The annealings at the temperature of 400°C for 4 and 6 h without external magnetic field improved the piezomagnetic properties (Figs. 4b, 5b and 7). After annealing at 500°C for 1/2 h in  $H_L$  there was observed a decrease of the  $k$  coefficient for the samples with a longer thermal treatment history, and the increase of the  $k$  (up to 0.45) for the sample no. 4, annealed

before only once. After the next annealing at 500°C for 1/2 h without magnetic field ( $H=0$ ) the maximum values of the  $k$  dropped to 0.3. The annealings for times longer than 1/2 h, e.g. 1 h, give the best results in the temperature range from 440 to 480°C (Fig. 10). In this range the decrease of the magnetostriction is not so sharp and the increasing of the magnetic permeability is observed (Fig. 10). The elasticity moduli changed from 75 to 200 GPa (Figs. 5, 8, 10) and the ultrasound velocities from about 3000 m/s to 5200 m/s, (see e.g. Figs. 6, 7, 9). A nanocrystallization occurred after next annealing for 1/2 h at the temperature of 550°C (Figs. 3 and 13). The magnetostriction in this alloy in the nanocrystalline state drops to the value below  $2 \times 10^{-6}$  [1, 5–8]. The saturation induction is equal to 1.15 T, the coercive force is lower than 1 A/m [1–8, 13]. When the magnetostriction vanishes or falls to very low values after thenanocrystallization, the soft magnetic properties become the best [1–8] but not the piezomagnetic parameters which are very bad [13] and the magnetomechanical coupling drops to nearly zero values. This alloy in the amorphous state and after the special heat treatment (annealing over the Curie temperature, which removes the most of the internal stresses) is better than the more expensive traditional nickel or other piezomagnetic materials [16–20]. However, its magnetomechanical coupling coefficient, which is two times larger than that of nickel, is lower than that observed in the iron rich Fe–Si–B metallic glasses [20–22]. The formation of nanocrystalline structure is ascribed to the combined addition of Cu and Nb which both are not soluble in  $\alpha$ -Fe. Hereby copper enhances the nucleation of  $\alpha$ -Fe grains, whereas the niobium lowers its growth rate [1–8]. The grain sizes after annealings in the range from 500 to 600°C for 1 h are about 10 to 15 nm [6–8]. From the piezomagnetic investigations it is seen (Fig. 10) that the nanocrystallization begins at the temperatures lower than 500°C [11].

## References

- [1] Y. YOSHIZAWA, S. OGUMA and K. YAMAUCHI, *New Fe-based soft magnetic alloys composed of ultrafine grain structure*, J. Appl. Phys. **64**, 10, 6044–6046 (1988).
- [2] Y. YOSHIZAWA and K. YAMAUCHI, *Effects of magnetic field annealing on magnetic properties in ultrafine crystalline Fe–Cu–Nb–Si–B alloys*, IEEE Trans. Magn. **MAG-25**, 5, 3324–3326 (1989).
- [3] G. HERZER, *Grain structure and magnetism of nanocrystalline ferromagnetics*, IEEE Trans. Magn. **MAG-25**, 5, 3327–3330 (1989).
- [4] H.R. HILZINGER, *Recent advances in rapidly solidified soft magnetic materials*, J. Magn. Magn. Mater. **83**, 1–3, 370–374 (1990).
- [5] M. MÜLLER, L. ILLGEN, E. KOHLER, M. BARTH and H. GRAHL, *Nanocrystalline Fe–B–Si-base soft magnetic alloys*, Int. Symp. MASHTEC'90, Dresden, Collected Abstracts, vol. 2, p. 345 (1990).
- [6] M. MÜLLER, L. ILLGEN, E. KOHLER, M. BARTH and N. MATTERN, *The influence of the composition of nanocrystalline FeBSi/CuNb soft magnetic alloys*, European Magnetic materials and Applications Conference, EMMA, Digest Booklet, Dresden 1991, pp 69–70.

- [7] M. MÜLLER, L. ILLGEN, and N. MATTERN, *The influence of different Si/B and Cu/Nb contents on the structure and the magnetic properties in nanocrystalline FeBSi base alloys*, Soft Magnetic materials 10, Abstract Booklet, Dresden 1991, p. 88.
- [8] M. MÜLLER, N. MATTERN, L. ILLGEN, H. R. HILZINGER and G. HERZER, *The influence of partial substitution of Nb by refractory elements on the structure and on the magnetic properties in nanocrystalline soft magnetic FeBSi-CuNb alloys*, Third International Conference on Amorphous Metallic Materials, AMM III, Topolcianky Castle, 1992, Book of Abstracts, P. 16.
- [9] Z. KACZKOWSKI AND M. MÜLLER, *Dependence of elasticity moduli on magnetic bias field of the Fe<sub>73.5</sub>Cu<sub>1</sub>Nb<sub>3</sub>Si<sub>16.5</sub>B<sub>6</sub> alloy before nanocrystallization*, J. Magn. magn. Mater. **101**, 1-3, 21-23 (1991).
- [10] Z. KACZKOWSKI and M. MÜLLER, *Dependence of magnetomechanical coupling on magnetic bias field in the Fe<sub>73.5</sub>Cu<sub>1</sub>Nb<sub>3</sub>Si<sub>16.5</sub>B<sub>6</sub> metallic glass before nanocrystallization*, J. Magn. Magn. Mater. **112**, 1-2, 320-322 (1991).
- [11] Z. KACZKOWSKI, L. MALKIŃSKI and M. MÜLLER, *Some piezomagnetic properties of Fe<sub>73.5</sub>Cu<sub>1</sub>Nb<sub>3</sub>Si<sub>16.5</sub>B<sub>6</sub> alloy after transverse field annealings*, Third International Conference on Amorphous Metallic Materials, AMM III, Topolcianky Castle, 1992, Book of Abstracts, P 40.
- [12] D. FRAITOVA and Z. FRAIT, *Characterization of amorphous and nanocrystalline ferromagnets by ferromagnetic resonance and antiresonance*, J. Magn. Magn. Mater. **101**, 1-3, 29-31 (1991).
- [13] Z. KACZKOWSKI, *Magnetomechanical coupling in transducers*, Arch. Acoust. **6**, 4, 385-400 (1981).

method was. The theoretical background of this new method is presented. Both methods of conversion are compared with reference to their use in acoustics. The tests of parameters important in processing of acoustics signals performed on monolithic "delta-sigma" converters are reported. A digital procedure for evaluating the THD+N parameter is proposed.

### 1. Introduction

Contemporary means of digital processing of acoustic signals are very powerful. This power comes from developments in hardware (monolithic digital signal processors) and from developments in the theory of signal processing. Wide access to theoretically unlimited precision of digital processing evokes the need for inexpensive analog to digital conversion systems introducing low error.

The recent developments in microelectronic technology made possible a large scale production of integrated circuits performing the task of analog to digital (A/D) and digital to analog (D/A) conversion according to the so-called "delta-sigma" conversion technique, known also as "sigma-delta" or "one-bit" conversion. This technique is the most popular version of a larger defined method of "oversampling" conversion. The actual method is not new. It stems from the patent of C. Cutler (filed in 1954), describing a multibit implementation in vacuum-tube technology [6]. The first presentation of the one-bit version of this method comes from 1962 [7]. The authors called their method "delta-sigma modulation".

The delta-sigma conversion technique applies very well to monolithic implementation in CMOS technology, which is substantial for low cost mass production. However, such production has become practicable only recently.

Oversampling A/D converters supersede the systems with "classical" A/D converters in most of the applications requiring high resolution of 16 bits or more. Achieving